

# Remote Pollution Probing by Laser-Induced Luminescence Techniques

Richard E. Grojean, John A. Sousa, Joseph F. Roach,  
 Elliot F. Wyner and Masato Nakashima  
 U. S. Army Natick Research and Development Command  
 Clothing, Equipment and Materials Engineering Laboratory  
 Natick, Massachusetts 01760

## Abstract

The general problem of remote detection for laser stimulated luminescent systems is considered. A simple optical model is employed to calculate the maximum practical range of detection for several such luminescent systems. Some experimental verification of the model is included. Consideration is also given to the practicality of using such a system for the remote detection of casual oil spills. The results of this study indicate that laser-induced fluorescence is a practical technique for the remote detection of pollutants. The ranges calculated from the simplified model are, in general, greater than those reported in the literature, but appear to be realizable.

## Introduction

It has been demonstrated recently<sup>1-7</sup> that numerous organic molecular systems, among which are several common pollutants, can be made to luminescence strongly under the action of continuous laser illumination. Such luminescence studies have been confined primarily to the laboratory; however, it has been demonstrated that laser-induced luminescence might be used for remote monitoring of certain pollutants. One such pollutant, which is sufficiently luminescent for this type of detection, is the casual oil spill.

In principle, remote monitoring of oil spills could be done at satellite distances. With the advent of space labs and space shuttles, sufficiently large monitoring systems could be constructed in space for the automatic detection and monitoring of oil spills before they are completely dispersed. Since a thick oil slick will disperse rapidly, reaching monomolecular thickness in a matter of hours, real time monitoring is essential. Once a slick is detected, closer surveillance could be maintained by smaller systems in aircraft. In this paper, we consider some of the parameters involved in the analysis and design of a model system, and report some results from an attempted experimental verification of this model.

## Optical Model

The optical model of such systems is basically the same as that for a lidar system. There are, however, minor differences in the photometric problem since the luminescent source is Lambertian in character (Figure 1) and there is a wavelength transformation due to the mechanism of luminescence.

The form of the equation for the power received at the photodetector from the laser stimulated luminescent source is

$$P_p = \int_{A_s} \int_{A_d} (T_d T_L \gamma P_L \cos\theta \cos\beta \exp(-(\sigma_l + \sigma_L)R)) dA_s dA_d / A_s \pi R^2 \quad (1)$$

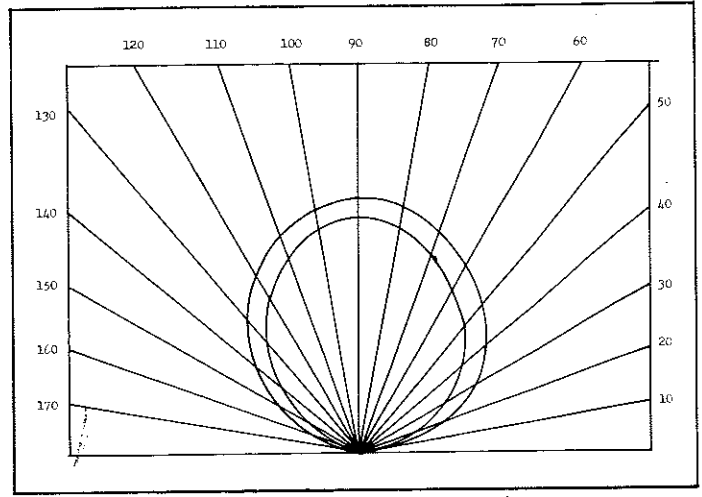


Figure 1. Angular distribution of luminescence from dyed fabrics.

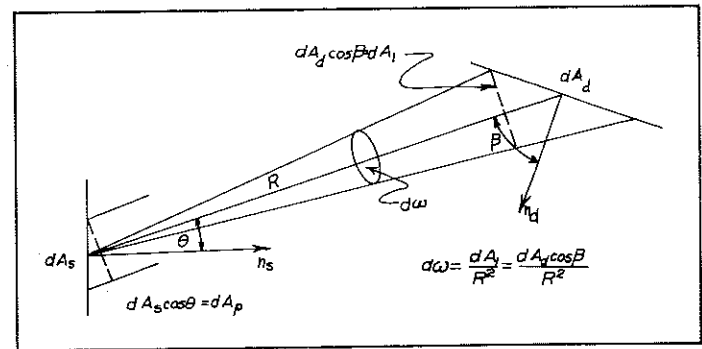


Figure 2. Geometry for the range equation.

(See Figure 2).

If we assume

$$R^2 \gg d_{A_s}, R^2 \gg d_{A_d}, \cos\theta = \cos\beta = 1 \quad (2)$$

and L constant over  $A_s$ ; to this degree of approximation we have

$$P_p = (T_d T_L \gamma P_L A_d \exp(-(\sigma_l + \sigma_L)R)) / \pi G R^2 \quad (3)$$

where

- $T_d$  is the transmission of the detector optics
- $T_L$  is the transmission of the laser optics
- $\gamma$  is the conversion efficiency from incident laser power to emitted luminescence
- $P_L$  is the power output of the laser
- $A_d$  is the clear aperture of the detector optics
- $\sigma_L$  is the atmospheric attenuation coefficient for the laser wavelength [ $\sigma = \sigma(\text{Rayleigh}) + \sigma(\text{Mie})$ ]

1406 received October 5, 1976; revised January 14, 1977.

$\sigma_q$  is the atmospheric attenuation coefficient for the luminescence wavelength (average over the band)  
 R is the range  
 $P_p$  is the power received at the photodetector  
 $G$  is a geometric factor for cases where the target does not fill the field of view.

This expression gives the power received at the photodetector as a function of the range of detection R.

**Calculated Distances of Detection vs Photocathode Current**

The maximum practical range for detection can be found by comparing the results of the range Eq. (3) with the minimum detectable signal for practical photodetectors. The practical lower limit of detectable signal will be set by the noise of the system. This noise (and here we define a noise signal as any unwanted signal that limits the desired signal) will have two origins, electronic and optical.

The detector we will consider in these calculations is a GaAs photomultiplier. The mean cathode dark current is  $3 \times 10^{-14}$  A/cm<sup>2</sup> while the radiant cathode sensitivity is 40 mA/watt.<sup>9</sup>

For the case of CW laser excitation of the fluorescent source, the limiting electronic noise will be given by

$$I_n = 2ei_0B \text{ (rms) and } i_0 = ne/T \tag{4}$$

where e is the electronic charge ( $1.6 \times 10^{-19}$  C)  
 $i_0$  is the time average of the emission or dark current and  
 B is the bandwidth of the measuring electronics;  
 $B > 0.5/T$  where T is the time constant.

For our system, T = 1 sec. The limiting noise is calculated to be

$$I_n = 2ei_0B \tag{5}$$

$$I_n = 7.55 \times 10^{-17} \text{ A}$$

The signal is given by

$I_s = \beta P_p$  where  $\beta$  is the radiant sensitivity of the photocathode. For this calculation we take  $I_s/I_n = 1$  as the limit. Note that  $I_n = C$  (const.) and is not a function of R if negligible optical "noise" is assumed.

With the above information, the photocurrent of the detector can be calculated as a function of distance up to the noise limit; in this case  $\sim 10^{-16}$  amp. This was done for a variety of samples and is presented in Figure 3. The parameters of the ex-

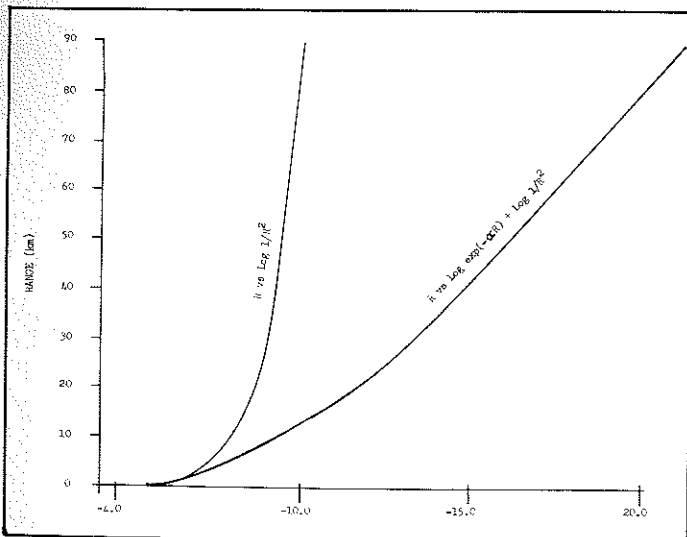


Figure 3. The separate effects of distance and scattering on the detection of luminescence as derived from Eq. (1).

periment were as follows:

$G$  = geometrical factor = 1 (target was larger than laser beam diameter)

- $T_L = 1$
- $T_d = 0.7$
- $\gamma$  = conversion efficiency of laser power to luminescence
- $P_L = 5 \times 10^{-3}$  W
- $A_d = 126 \text{ cm}^2$  (5 inch aperture)
- $\text{COS } \beta = 1, (\beta=0)$
- $\sigma_L = 0.15/\text{km}^2$
- $\sigma_q = 0.14/\text{km}^2$
- $\beta = 4 \times 10^{-2}$  A/W radiant cathode sensitivity

Substitution into the range equation gives

$$P_p = (1.40 \times 10^{-5}) (\exp(-0.29 \times 10^{-3} R)) \gamma / R^2 \text{ watts}$$

and the detector signal level is given by

$$I_s = \beta P_p$$

The  $\gamma$ 's were measured for the luminescent systems and the range of detection calculated. The results are presented in Table 1. For distances up to  $\approx 5$  km, the curves follow a  $1/R^2$  relation-

Table 1. Maximum Range of Detection

Luminescent System	I(mW)	$\gamma$	R (kilometers)
Dye System A	1	$9.36 \times 10^{-2}$	5.0
Dye System A	5	$9.36 \times 10^{-2}$	7.6
Dye System A	100	$9.36 \times 10^{-2}$	13.8
Dye System A	150	$9.36 \times 10^{-2}$	14.8
Dye System A	5000	$9.36 \times 10^{-2}$	24.1
Dye System B	5	$6.56 \times 10^{-3}$	3.6
Crude Oil #6	5	$1.29 \times 10^{-3}$	2.5

ship after which the exponential function dominates. The influence of each function on the intensity as a function of distance is shown in Figure 3. It can be seen that the maximum distance of detectability as the laser intensity is increased, is determined by the scattering function. Figure 4 represents the variation in range of detection of induced luminescence with laser intensity.

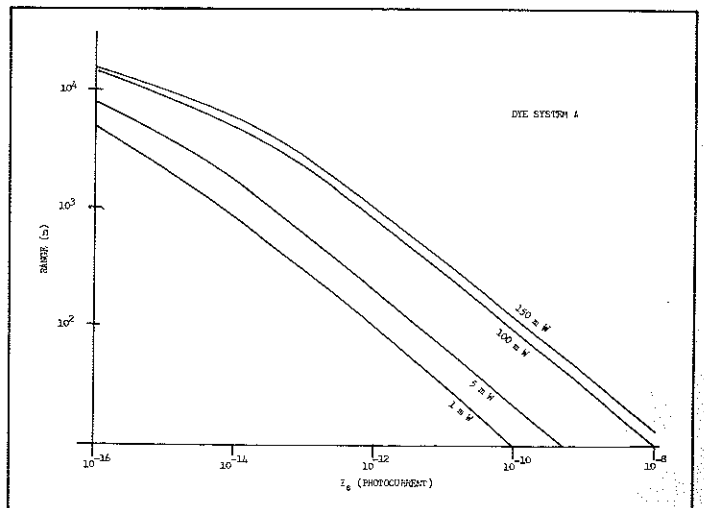


Figure 4. A typical change in detectability of luminescence for a change in laser intensity.

**Experimental Verification of the Range Equation**

In order to test the validity of the range equation, the model was checked by comparing calculated values of signal magnitude with actual tests employing the two dye systems as targets. The parameters were determined for each of the dye systems. They

Table 2. Experimental Data for Range Model

Parameter	Dye System A	Dye System B
G	1	3.1
$\gamma$	$9.3 \times 10^{-2}$ W/W	$6.6 \times 10^{-3}$
$T_d$	0.30	0.30
Laser light transmitted through filter	$9.2 \times 10^{-12}$ A	$4.5 \times 10^{-11}$ A
Range	145 m	73 m
Dark Current	$0.38 \times 10^{-9}$ A	$0.38 \times 10^{-9}$ A
Photometric reading	$8.4 \times 10^{-9}$ A	$1.25 \times 10^{-9}$ A

are listed in Table 2.

The filter rejection of laser intensity was measured as  $3 \times 10^{-3}$  from which the total amount of laser transmitted to the detector could be calculated and subtracted from the final reading. The phototube dark current was found by operating the system normally, but with a black cloth completely covering the target. Considering the above modifications, the signal obtained for each system was as follows:

$$I_A = 8.0 \times 10^{-9} \text{ A}$$

$$I_B = 8.3 \times 10^{-10} \text{ A}$$

The calculated value for each case is found to be  $I_A = 8.07 \times 10^{-9}$  A. Therefore,  $I_B = 7.01 \times 10^{-10}$  A.

There is a reasonable comparison of the values for the calculated case and the experimental data. The data lends credence to the derived range equation for the approximations and conditions imposed.

Experimental Data for Crude Oil

The corrected luminescence spectral data of crude oil #6 was obtained on the Perkin-Elmer Model MPF-3 fluorescence spectrophotometer using 337 and 364 nm as the excitation wavelengths (Figure 5). The luminescence spectra were also obtained

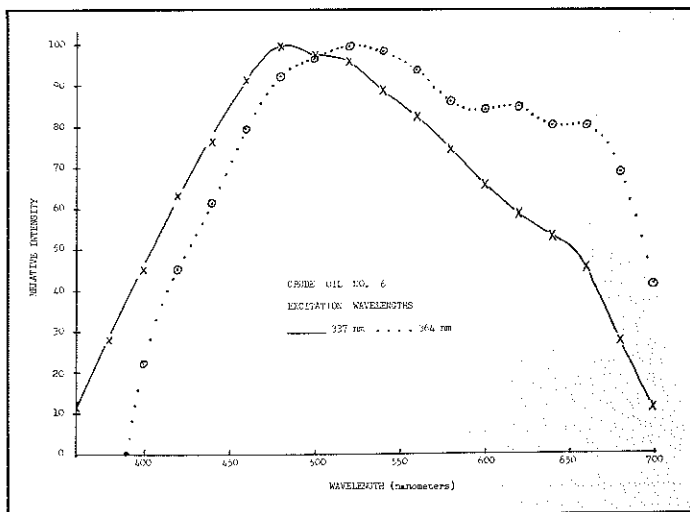


Figure 5. Crude Oil No. 6, excitation wavelengths, 337 nm and 364 nm.

as a function of luminescence power by exposure of the oil to laser light at 364 nm and is shown in Figure 6. Since the luminescence intensity covers the total visible spectrum, a bandpass filter was chosen to optimize the luminescence signal and to discriminate against ambient background.

By incorporating the various parameters in the range equation, the photocurrent of the detector system was determined

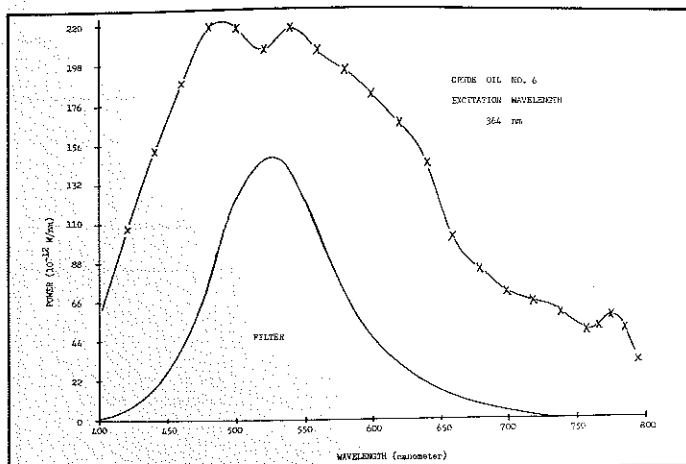


Figure 6. Crude Oil No. 6, excitation wavelength, 364 nm.

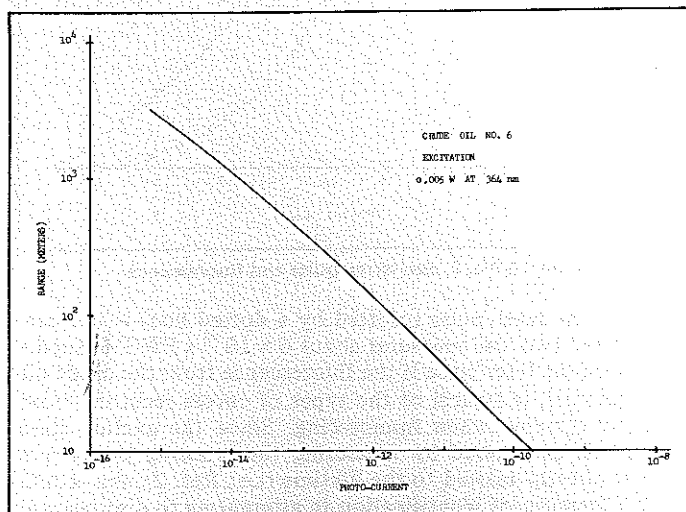


Figure 7. Crude Oil No. 6, excitation, 0.005 W at 364 nm.

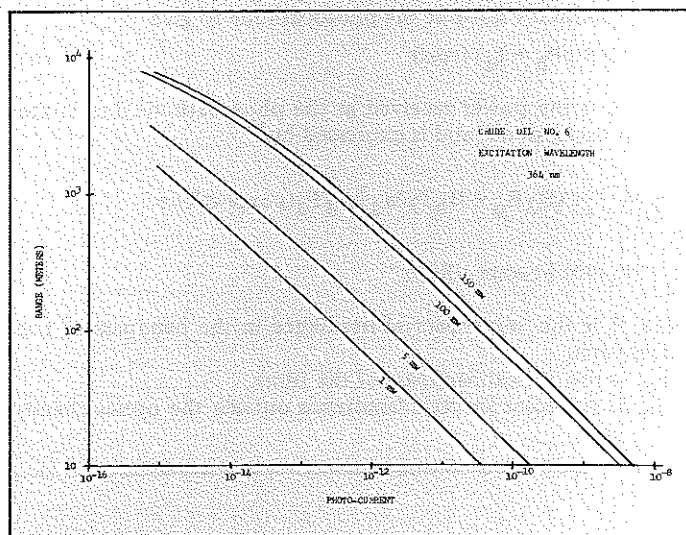


Figure 8. Crude Oil No. 6, excitation wavelength, 364 nm.

as a function of distance up to the detection limit, in this case  $\sim 10^{-16}$  A. From this data, the maximum range of detectability at various laser intensities was calculated as shown in Figures 7 and 8 and presented in Table 3.

Crude oil #6 was also irradiated by a pulsed dye laser, using the exciting wavelength of 364 nm. The pulse shape is shown in

**Table 3. Maximum Range of Detection**

Laser Power (mW)	R (kilometers)
1	1.3
5	2.5
100	6.3
150	7.1

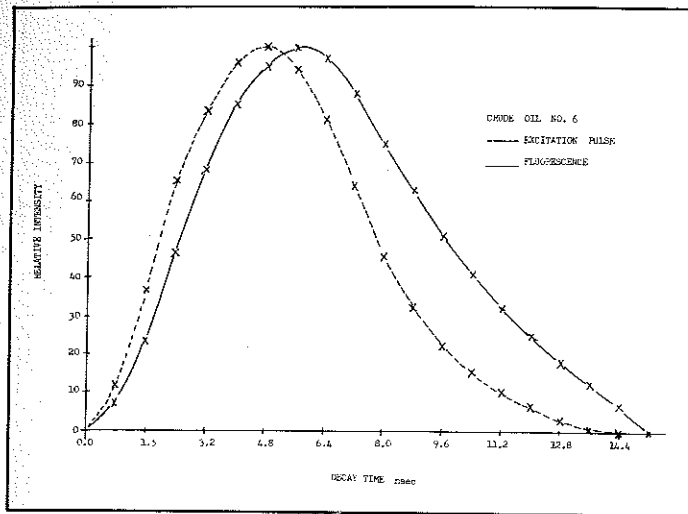

**Figure 9. Crude Oil No. 6, excitation pulse and fluorescence.**

Figure 9. The laser pulse (plotted by a dotted line) is the narrower of the two and measures about  $6 \times 10^{-9}$  s FWHM. Superimposed on the laser pulse is the fluorescence from the crude oil and, in general, is typical of the types of curves recorded from molecular systems when luminescing. Since the excited state lifetime can be studied by measuring the intensity decay rate which is directly related to the lifetime (i.e., Ref. 2), this would afford a measure of identification in attempting to discriminate against interfering backgrounds.

The noise due to an ambient background may be included in the expression for noise at the photocathode to give

$$I_n = 2eB(\beta P_b + I_d) \text{ (rms)} \quad (6)$$

where  $P_b$  is the power received at the photocathode due to the ambient background, and is expressed by<sup>10</sup>

$$P_b = \frac{1}{4} (H_\lambda B_o + H_b T_\lambda) a_d^2 A_d T_d (\rho \exp(-\sigma R) + (\sigma_s/4\sigma) [1 - \exp(-\sigma R)]) \quad (7)$$

where  $H$  is the solar spectral irradiance in the bandpass of the optical filter.

$B_o$  is the optical bandpass of the filter.

$H_b$  is the solar spectral irradiance outside the optical bandpass.

$T_\lambda$  is the relative transmission of the optical filter outside the bandpass.

$a_d$  is the angular field of the detector optics.

$A_d$  is the clear aperture of the detector optics.

$T_d$  is the transmission of the detector optics and filter (over  $B_o$ ).

$\rho$  is the reflectivity of the source.

$\sigma$  is the atmospheric attenuation coef.

$\sigma_s$  is the atmospheric back scattering coef.

The magnitude of the noise signal under daylight background illumination can now be calculated. Note that the first term in the square bracket represents reflected sunlight from the target, attenuated by the atmosphere. The second term gives the contribution of sunlight scattered by the atmosphere within the field of view of the detector. For the case of a 5 milliwatt laser, the range is such that the atmospheric attenuation and scatter are negligible. Assume the following data:

$B_o = 100$  nm centered at fluorescence max. = 700 nm

$T_d = 0.7$

$\sigma = 0.2/\text{km}$

$H_\lambda = 0.48 \text{ W/m}^2 \text{ nm}$

$H_b = 740 \text{ W/m}^2$

$T_\lambda = 10^{-6}$  (interference filter)

$\sigma_s = 0.21 \text{ km}$

$B = 0.5/\text{sec}$  (DC case  $\tau = 1$  sec)

$A_d = 126.6 \text{ cm}^2$

$a_d = 1$  mrad

$\rho = 0.1$

Approximately (neglecting atmospheric effects),

$P_b = H_\lambda B_o a_d^2 A_d T_d \rho / 4$

$P_b = 1.06 \times 10^{-9} \text{ W}$

and

$I_n = 2.6 \times 10^{-15} \text{ A}$

as compared to  $7.55 \times 10^{-17} \text{ A}$  for dark current alone.

This represents an order of magnitude decrease in the detection range. If the laser is now pulsed so that a matched electronic filter may be employed, the noise bandwidth may be reduced with negligible loss of signal. An increase in luminescence has been noticed as the pulse rate is increased.<sup>2,3</sup> This is particularly true for weakly luminescent systems. This phenomenon is under investigation and promises an increase in detection range approaching an order of magnitude for some molecular systems.

## References

1. E. F. Wyner, J. A. Sousa, J. F. Roach, and M. Nakashima, *American Dyestuff Reporter*, November 1973.
2. E. F. Wyner, J. A. Sousa, and J. F. Roach, *Spectroscopy Letters*, Vol. 8, No. 7 (1975).
3. R. E. Grojean, Final Report, US Army Research Office, Durham, Grant No. DAHCO4 74G 0042.
4. R. M. Measures, W. Houston, and M. Briston, *Canadian Aeronautics and Space Journal*, Vol. 19, No. 10 (1973).
5. H. H. Kim, *Applied Optics*, Vol. 12, No. 7 (1973).
6. A. W. Tucker, M. Birnham, and C. L. Fincher, *Applied Optics*, Vol. 14, No. 6 (1975).
7. J. T. Fantasia, T. M. Hard, and H. C. Ingras, DOT-TSC Report 71-7.
8. *Chemical Rubber Company Handbook of Lasers*, (1971).
9. *RCA GaAs Photomultiplier Data Sheet*.
10. *RCA Electro-Optics Handbook* (1968).